Decoding Sensory Feedback From Firing Rates of Afferent Ensembles Recorded in Cat Dorsal Root Ganglia in Normal Locomotion

Douglas J. Weber, Richard B. Stein, Dirk G. Everaert, and Arthur Prochazka

***Abstract*—Sensory feedback is required by biological motor control systems to maintain stability, respond to perturbations, and adapt. Similarly, motor neuroprostheses require feedback to provide natural and complete restoration of motor functions. In this paper, we show that ensemble firing rates from the body's mechanoreceptors can provide a natural source of kinematic state feedback and could be useful for prosthetic control. Single unit recordings from multiple primary afferent neurons were obtained during walking using multichannel electrode arrays implanted chronically in the L7 dorsal root ganglia of three cats. We typically recorded simultaneously from over 20–30 neurons during the first 7–14 days after surgery, but recordings gradually worsened thereafter. Histology indicates that a ring of inflammatory and connective tissues (100 μm thick) develops around each microelectrode and likely contributes to the degradation in recording quality. Accurate estimates of the hindlimb trajectory were made using a linear filter with inputs from only a few neurons highly correlated with limb kinematics. The coefficients for the linear filter were identified in a least-squares fit with 5–10 s of walking data (model training stage). The estimated and actual trajectories of separate walking data generally match well for walking at a range of speeds accounting for $63 \pm 22\%$ (mean $\pm$ S.D. for hip, knee, and ankle) of the variance in joint angle and $72 \pm 4\%$ of the variance in joint angular velocities. These results indicate that a neural interface with primary sensory neurons in the dorsal root ganglion can provide accurate kinematic state information that may be useful for closed loop control of a neuroprosthesis.**

***Index Terms*—Cat, chronic recording, locomotion, microelectrode array, neuroprosthesis, sensory neurons.**

I. Introduction

Many different research groups are developing neural interface technologies to provide command signals for directing a wide range of tasks including cursor movement, robotic arm control, and functional electrical stimulation [1]–[5]. For complex control tasks such as reaching and walking, sensory feedback is required to maintain stability and monitor the kinematic state (i.e., position and velocity) of the controlled limb. A natural source of kinematic and kinetic state information is the group of mechanosensory neurons (e.g., muscle spindles, golgi tendon organs, joint receptors, and cutaneous afferents) that normally mediate proprioception [6], [7].

We are testing the feasibility of extracting hindlimb position and velocity information during walking using ensembles of sensory afferents chronically recorded in the L7 dorsal root ganglion (DRG) of walking cats. The gathering together of afferent cell bodies within the DRG provides a convenient location for using microelectrode recording techniques to gain access to the entire suite of mechanosensory modalities. Approximately 30 years ago, Prochazka *et al.*, [8] and Loeb *et al.*, [9], independently developed techniques to implant microwires into the DRG to record from sensory afferents in awake, behaving cats. These experiments provided the first records of hindlimb afferent activity in the freely moving animal and revealed the natural patterns of afferent discharge that contribute to reflexes and proprioception.

Loeb *et al.* [9] immediately realized that these proprioceptive signals could provide useful feedback for controlling a neural prosthesis, but noted that improvements were needed to extend the recording life and capacity of the implanted electrodes. Since then, a variety of neural interface technologies have been developed for chronic recording of nerve signals. In fact, cuff electrodes are now being used to record compound sensory potentials for gait event detection in human foot drop stimulator applications [6], [10]. An advantage of using epineural electrodes is that they are relatively easy to implant and the signal processing requirements are straightforward since single unit spike discrimination is not required. However, the electrodes are nonselective and the recorded signals provide only composite records of multineuronal activity from primarily the largest nerve fibers. As a result, whole nerve recordings have only been used for detecting discrete events such as ground contact time in the foot drop application [6]

More complex neuroprosthetic applications may require continuous state feedback to provide an adaptive controller that can detect and respond to perturbations. Results from acute studies in anesthetized cats show that continuous position and velocity information can be extracted from ensembles of single unit sensory afferents recorded in the dorsal root ganglion (DRG) [11]. In this report, we demonstrate in chronic experiments with behaving animals the feasibility of 1) recording and discriminating the spiking activity of many afferent neurons simultaneously, and 2) extracting continuous position and velocity information from the activity of an ensemble of afferents.

Penetrating microelectrode arrays (9×4 grid, Cyberkinetics, LLC) were chronically implanted into the left L7 dorsal root ganglion of three adult cats and afferent recordings were made during treadmill walking. Multivariate regression models were used to study correlations between ensemble afferent activity and the kinematics of the ipsilateral hindlimb. There were strong linear correlations between afferent activity and limb kinematics. Joint positions and velocities were accurately estimated using simple linear combinations of firing rates from as few as ten afferent neurons. Thus, a straightforward weighted summation of firing rate signals from a small ensemble of afferents is sufficient to estimate limb kinematic variables during walking and, in principle, this could provide useful kinematic state feedback for a motor neuroprosthesis.

II. Methods

All procedures were approved by the University of Alberta, Edmonton, AB, Canada, animal policy and welfare committee. In each of five cats, a sterile surgery was performed to implant a microelectrode array into the L7 DRG for chronic neural recording during normal treadmill locomotion. In two cats, we experienced technical problems with wire and insulation breakage and were unable to obtain neural recordings during walking.

A. Chronic Microelectrode Array Implantation in DRG

A 9×4 microelectrode array (Cyberkinetics, Foxboro MA) was implanted into the L7 DRG under aseptic conditions and isoflurane anesthesia. The microelectrodes were 1.5 mm in length and spaced 400 μm apart. A bundle of gold lead wires (10 cm long, 20 μm diameter, Isonel insulation) connected the electrodes to a percutaneous connector. The electrode impedances were between 100 and 1000 kΩ when tested with a 1000-Hz sinusoidal current (~ 0.5 μA rms).

The back was shaved and a skin incision was made along the midline of the back from the L5 to S2 spinous processes. Paraspinal muscles

Manuscript received August 17, 2005; revised March 22, 2006. This work was supported in part by the Canadian Institutes of Health Research and in part by the Alberta Heritage Foundation for Medical Research.

D. J. Weber was with the University of Alberta, Edmonton, AB, T6G 2H9, Canada. He is now with the Department of Physical Medicine and Rehabilitation, University of Pittsburgh, Pittsburgh, PA 15213 USA (e-mail: djw50@pitt.edu).

R. B. Stein, D. G. Everaert, and A. Prochazka are with the University of Alberta, Edmonton, AB, T6G 2S2, Canada (e-mail: richard.stein@ualberta.ca; everaert@ualberta.ca; arthur.prochazka@ualberta.ca).

Digital Object Identifier 10.1109/TNSRE.2006.875575

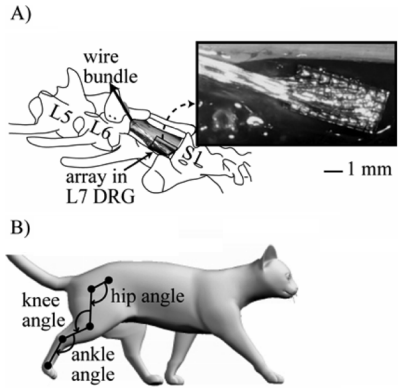

Fig. 1. Experimental setup. (A) Microelectrode array chronically implanted in L7 DRG. Picture inset shows an enlarged view of the implanted array. (B) Hip, knee, and ankle joint angles were calculated by tracking the positions of five markers placed over iliac crest, hip, knee, ankle, and MTP joints.

overlying the transverse processes of L5 to S1 vertebrae were resected to expose the laminae. A laminectomy was performed at the L7 segment to expose the spinal cord and dorsal roots. The dura was left intact. A small length of a 4-0 suture needle was hooked through the L6 spinous process to provide an anchor to the bone and a layer of dental acrylic was formed around this and the spinous process serving as a fixation point for the wire bundle.

When the electrode array was properly positioned over the center of the L7 ganglion, the gold wires were glued to the L6 acrylic cap using cyanoacrylate [see Fig. 1(A)]. Next, the array was inserted into the DRG through the dura using a pneumatic tool that applies an impulsive force to the array substrate for rapid insertion [12]. Two platinum reference wires were placed in the epidural space of the spinal canal.

B. Multichannel Neural Recording

The methods used for recording and discriminating single units are described in [11]. However, we modified the recording hardware to increase the cutoff frequency for the highpass filter from 250 to 1500 Hz to reduce electromyogram (EMG) contamination. Occasionally, we used a series of tests to identify units by their receptor type (e.g., muscle spindle, cutaneous) and receptive field location. The unit identification procedure is described in [11] but was only performed in about 30% of all recording sessions as it requires anesthetizing the cat.

C. Kinematics

Each behavioral experiment was videotaped using a high-speed digital (120 Fields-s^{-1}) video camera (GRDV9800, JVC Corporation). Kinematic and neural data records were aligned to the onset-time of a light-emitting diode (LED) placed in the camera view. The voltage signal powering the LED was recorded by the neural data acquisition system at a sampling rate of 1000 samples-s^{-1}. The rising edge of the LED voltage was aligned with the video frame first showing the illuminated LED.

White markers were glued to the skin over the iliac crest, and the joint centers of the hip, knee, ankle, and metatarsophalangeal (MTP) joints, as shown in Fig. 1(B). The centroid of the marker was automatically located in each image of the video using custom MATLAB (Mathworks, Inc.) software. The camera plane was parallel to the sagittal plane of the leg. Calibration markers were spaced 10 cm apart in the horizontal and vertical planes and used to calibrate the camera view. Parallax errors were compensated by scaling the segment vectors by the measured separation distance between the ankle and MTP markers (i.e., foot length which is constant).

Hip, knee, and ankle joint angles were computed from the digitized marker positions, extension corresponding to a positive angular displacement. The knee marker was not used, because the skin overlying the knee tends to slide over the joint during locomotion. Instead, the knee-joint angle was calculated using (1), which follows from the law of cosines

$$\theta_{\text{knee}} = \cos^{-1}\left(\frac{L_{\text{femur}}^2 + L_{\text{shank}}^2 - d^2}{2 \cdot L_{\text{femur}} \cdot L_{\text{shank}}}\right). \tag{1}$$

The three distances used in this calculation are: 1) L_{femur} : femur length; 2) L_{shank} : shank length; 3) d : distance between the hip and ankle markers.

D. Neural Decoding Model

Instantaneous firing rates for each neuron were computed at 8.3 ms intervals corresponding to the sample times of the kinematics. Equation (2) shows the linear filter used to convert the discrete spike events into a uniform time series of firing rates. This filter is noncausal and has a triangular kernel providing an unbiased estimate of firing rate that scales the contribution of each spike by its distance from the time-point of interest [11]

$$f_i = \frac{1}{\Delta t}\sum_j \left(1 - \frac{|t_i - t_j|}{\Delta t^2}\right). \tag{2}$$

In (2), the firing rate (f_i) is computed at each time index i, t_i is the current time, t_j is the jth spike in the interval $[t_i - \Delta t, t_i + \Delta t]$, and Δt is the sampling interval (8.3 ms). A second order resistance–capacitance (*RC*) filter ($\tau = 100$ ms) was used to smooth the firing rates and kinematic variables as described in [11].

Hindlimb trajectories were estimated from the ensemble of neural activity using the linear filter model shown in (3)

$$\hat{\mathbf{Q}}_i = \mathbf{Bo} + \sum_{j=0}^{k} \mathbf{B}_j \mathbf{F}_{i-j} \tag{3}$$

where: $\hat{\mathbf{Q}}_i$ is the estimated limb state vector (i.e., hip, knee, and ankle joint angles and angular velocities) at time index i, **B** is the coefficient matrix, and **Bo** is a vector of bias terms (intercepts). The duration of signal over which the filter window operates is defined by the maximum lag variable k (e.g., 12 bins $=$ 100 ms) and $\mathbf{F}_{i-j}$ is the vector of filtered firing rates at time index $i - j$. Summation over the k lag times includes all firing rates in the interval $[t_{i-j}, t_i]$. The variance-accounted-for (VAF or R^2) was used to assess the quality of the estimation for each variable. Since the decoding model yields both position and velocity predictions, we combined the position and velocity predictions to improve the path estimation using (6) in [11].

Each of the six state variables was decoded from the firing rates of ten neurons using (3). To select neurons for decoding, the unsigned correlation coefficient between each state variable and afferent firing rate was calculated. The ten neurons with the highest correlation coefficients for each state variable were used in the decoding model. Thus, different groups of neurons may be used to decode the six state variables.

Once the neurons were selected, the coefficients [**Bo** and **B** in (3)] were calculated through a least-squares fit. 5–10 s of walking data were used in the model identification (training) stage. Separate walking data were used to test the performance of the model. All of the results presented are from "test" data sets with 5–12 steps.

III. Results

A total of five adult cats were implanted with 9×4 arrays of electrodes. Within the first six days after surgery, the numbers of recorded

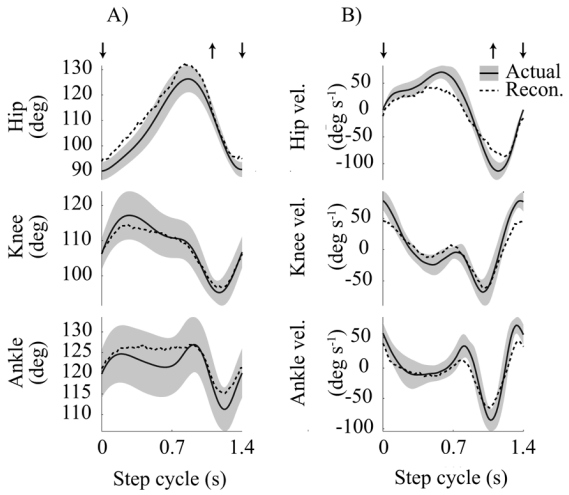

Fig. 2. Actual and estimated joint trajectories averaged over ten sequential steps (heel-strike to heel-strike). Shaded regions represent ± 1 S.D. from the mean of the actual trajectories. (A) Hip, knee, and ankle joint angles, and (B) angular velocities. VAF in the hip, knee, and ankle angle estimations are 73%, 78%, and 37%, respectively. The VAF in the corresponding angular velocity estimations are 76%, 69%, and 71%. Heel-strike and toe lift-off times are indicated by the down and up arrows, respectively. Data taken from cat A.

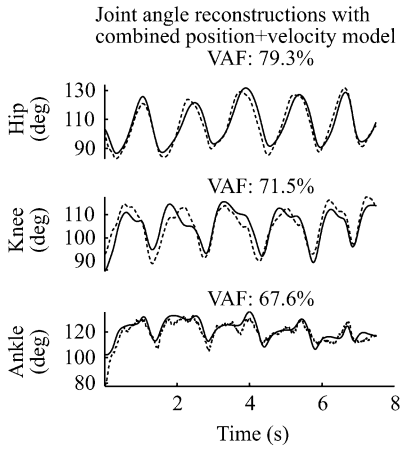

Fig. 3. Joint angle estimates using combined (position+ velocity) model. This analysis was based on data from cat C.

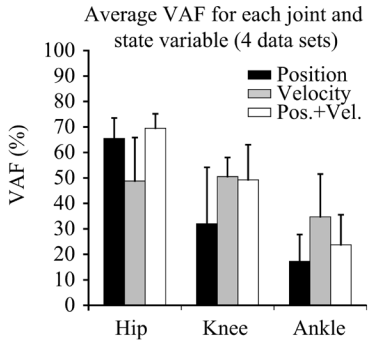

Fig. 4. Average VAF by the decoding models. Errorbars denote 1 S.E. Position, velocity, and combined position+velocity model results are shown. Data from all three animals (A, B, and C) was used for this analysis, but two different data sets were taken from separate recording days with cat A.

units in each cat were: $13 \pm 3, 13 \pm 8, 25 \pm 5, 23 \pm 6$, and 36 ± 13 $(\text{mean} \pm \text{S.D.})$. In the first two animals, technical problems precluded long-term recording from a large number of units while the animals were walking. In the other three animals (labeled A, B, and C), we were able to record from substantial numbers of units (daily average 23 ± 9) for 2–5 weeks and results presented are from these three animals.

A. Neural Decoding During Treadmill Walking

Neural and kinematic data were recorded during treadmill locomotion. Approximately ten trials (walking for 60 s) were recorded during each session. We restricted our analysis to segments of data where the cat walked for 5–10 consecutive steps without turning sideways or sitting down. Treadmill walking speeds ranged from 0.2 to 0.5 m s^{-1}, but the typical speed was 0.4 m s^{-1}.

The linear decoding model in (3) was used to estimate the joint-space kinematics from the firing rates of small groups of afferents ($\{n\} = 10$). Fig. 2 shows an example of actual and estimated trajectories of joint angle (A) and angular velocity (B) averaged over ten sequential step cycles (heel-strike to heel-strike). Ten neurons were used in these estimations and the decoded and actual trajectories generally matched well. The decoding estimates accounted for $63 \pm 22\%$ (mean $\pm$ S.D. for hip, knee, and ankle) of the variance in joint angle and $72 \pm 4\%$ of the variance in joint angular velocities. The average root mean square (rms) error in the joint-angle estimations was $6.6 \pm 2^\circ$ and $27 \pm 3^\circ$ s^{-1} in angular velocities. Among the ten neurons used in the estimate, one was a hamstring muscle spindle Ia afferent, which likely explains the accuracy of the hip and knee estimates. The largest error was in the ankle angle during the stance phase when the ankle extensor muscles are active, but the ankle "yields" into flexion. The angle and angular velocity estimates for the knee and hip are excellent throughout the step cycle.

These data indicate that the sensory afferent activity is highly correlated with position and velocity variables. The position and velocity estimates were combined to refine the joint position estimates (see [11, eq. 6]). Fig. 3 shows actual and estimated joint positions during a series of 5 steps (cat C) using the combined (position + velocity) model. Overall, the path estimates closely match the actual trajectories, with the average VAF for both coordinate systems exceeding 70%.

Decoding analyses were done with four different data sets and the VAF scores for each state variable were averaged to compare the quality of the position, velocity, and position + velocity estimates (see Fig. 4). For the knee and ankle, the VAF for the angular velocity variables was much stronger than the corresponding angular position variables. The angular position estimates were improved by an average of 9% VAF using the combined position + velocity model.

The hip angle was most strongly correlated with the afferent activity, the group average VAF exceeding 65%. This is interesting given that most of these L7 afferents had their receptive fields in the distal part of the limb (around the knee, ankle, and MTP joints and in the toepads). The weakest correlations were with ankle angle, which is not surprising, given that the contributing units also responded to movements of the toes in some cases, and given the likelihood of variations in fusimotor drive coupled to muscle activation levels. Although the ankle dorsiflexes more during the swing phase than the stance phase, there is no toe dorsiflexion and there is probably less fusimotor drive to spindles in the inactive muscle [13].

IV. Discussion and Conclusion

Mechanosensory afferent neurons are a potential source of kinematic state feedback for controlling neuroprosthetic systems. This paper demonstrates the feasibility of 1) recording from large numbers of primary afferents in a freely behaving cat, and 2) accurate estimation of position and velocity variables from the firing rates of a select group of afferents highly correlated with limb kinematic variables.

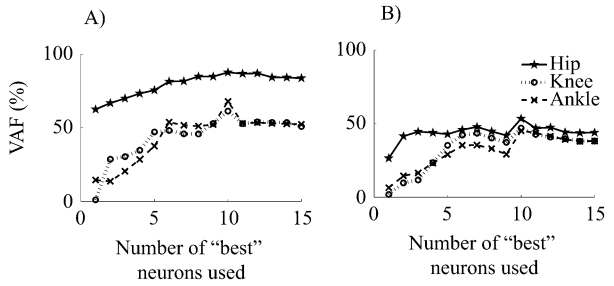

Fig. 5. Decoding performance (VAF) varies with the number of units used in the decoding models for position (A) and velocity (B). VAF values for hip, knee, and ankle kinematics are shown. "Best" units are ranked by their correlation with the state variables. This analysis was based on data from cat C.

Recording from large numbers of sensory afferents is crucial to obtain sensory representations for the entire limb (i.e., three joints) and kinematic state space (i.e., position and velocity). The linear filter models used here comprised simple linear combinations of afferent signals to estimate limb kinematics and likely represent the minimum in achievable performance. Obviously, these models are not able to represent nonlinear properties of the sensory response or nonstationarities produced by changes in fusimotor drive to muscle spindles. These limitations may contribute to estimation errors in the ankle-joint angle and angular velocity (see Fig. 2). Nevertheless, linear filtering provided reasonably accurate estimates of the hindlimb kinematics using firing rates from only ten neurons.

Although we typically obtained simultaneous recordings from more than 20 neurons, we chose to use only ten neurons in the decoding model. The optimal number of neurons to use obviously depends on the encoding properties of the neurons recorded, because neurons poorly correlated with limb kinematics will not improve the decoding performance. In a previous report [11], we showed that decoding accuracy increases with the number of neurons used in the model, but using more than ten neurons does not significantly improve the VAF or decoding error. Prochazka and Gorassini [14] also reported that firing rate profiles from five or six muscle spindles are sufficient to describe the afferent ensemble response.

Fig. 5 shows an example of the relationship between decoding performance (VAF) and the number of neurons used in the decoding model with data from cat C. The VAF for all state variables increases gradually and reaches a maximum when ten neurons are used. Using more than ten neurons actually results in a small decrease in the VAF, likely caused by the inclusion of neurons weakly correlated with the state variables.

Finally, chronic recording stability is an important requirement for developing a stable sensory neural interface for neuroprosthetic applications. The useful recording lifespan of the chronic microelectrodes used in these experiments was typically 7–21 days during which time 20–30 neurons could be discriminated daily. In all cases, the recording quality gradually degraded thereafter.

Histology indicates that a ring of connective tissue (100 μm thick) develops around each microelectrode and likely contributes to the degradation in recording quality, but neuronal death in the region surrounding the microelectrode may also contribute to the loss of neural recordings. Systematic studies of the potentially many factors that could be limiting the long-term viability of chronic recording electrodes are needed to characterize the failure modes and test interventions for preventing electrode encapsulation and cell death.

It will also be important to characterize the day-to-day variation in the neurons recorded. For this approach to be practical for neuroprosthetics applications, the sampled population of afferents should be stable to provide consistent feedback signals. If a stable and reliable interface can be developed, the results presented here indicate that meaningful information about limb state can be derived from primary sensory neurons in the dorsal root ganglion. Therefore, a DRG-based sensory neural interface would provide useful kinematic state feedback for closed loop control of a neuroprosthesis.

ACKNOWLEDGMENT

The authors would like to thank R. Rolf for providing technical assistance with the neural recording hardware, the animal technicians in the HSLAS at the University of Alberta, and L. Sanelli and K. Todd for technical assistance with the histology.

REFERENCES

[1] M. D. Serruya, N. G. Hatsopoulos, L. Paninski, M. R. Fellows, and J. P. Donoghue, "Instant neural control of a movement signal," *Nature*, vol. 416, pp. 141–2, 2002.

[2] D. M. Taylor, S. I. Tillery, and A. B. Schwartz, "Direct cortical control of 3D neuroprosthetic devices," *Science*, vol. 296, pp. 1829–32, 2002.

[3] J. R. Wolpaw, N. Birbaumer, W. J. Heetderks, D. J. McFarland, P. H. Peckham, G. Schalk, E. Donchin, L. A. Quatrano, C. J. Robinson, and T. M. Vaughan, "Brain-computer interface technology: A review of the first international meeting," *IEEE Trans. Rehabil. Eng.*, vol. 8, no. 2, pp. 164–73, Jun. 2000.

[4] R. T. Lauer, P. H. Peckham, K. L. Kilgore, and W. J. Heetderks, "Applications of cortical signals to neuroprosthetic control: A critical review," *IEEE Trans. Rehabil. Eng.*, vol. 8, no. 2, pp. 205–8, Jun. 2000.

[5] J. A. Hoffer, R. B. Stein, M. K. Haugland, T. Sinkjaer, W. K. Durfee, A. B. Schwartz, G. E. Loeb, and C. Kantor, "Neural signals for command control and feedback in functional neuromuscular stimulation: A view," *J. Rehabil. Res. Dev.*, vol. 33, pp. 145–57, 1996.

[6] M. Haugland and T. Sinkjaer, "Interfacing the body's own sensing receptors into neural prosthesis devices," *Technol. Health Care*, vol. 7, pp. 393–9, 1999.

[7] D. J. Weber, R. B. Stein, A. Prochazka, and R. A. Normann, "Progress toward a neural interface for feedback control of a neuroprosthesis," presented at the Soc. Neurosci. Annu. Meeting, New Orleans, LA, 2003.

[8] A. Prochazka, R. A. Westerman, and S. P. Ziccone, "Discharges of single hindlimb afferents in the freely moving cat," *J. Neurophysiol.*, vol. 39, pp. 1090–104, 1976.

[9] G. E. Loeb, M. J. Bak, and J. Duysens, "Long-term unit recording from somatosensory neurons in the spinal ganglia of the freely walking cat," *Science*, vol. 197, pp. 1192–4, 1977.

[10] J. A. Hoffer, M. Baru, S. Bedard, E. Calderon, G. Desmoulin, P. Dhawan, G. Jenne, J. Kerr, M. Whittaker, and T. J. Zwimpfer, "Initial results with fully implanted Neurostep FES system for foot drop," in *Proc. X IFESS Annu. Meeting*, Montreal, QC, Canada, 2005.

[11] R. B. Stein, D. J. Weber, Y. Aoyagi, A. Prochazka, J. B. Wagenaar, S. Shoham, and R. A. Normann, "Coding of position by simultaneously recorded sensory neurones in the cat dorsal root ganglion," *J. Physiol.*, vol. 560, pp. 883–96, 2004.

[12] P. J. Rousche and R. A. Normann, "A method for pneumatically inserting an array of penetrating electrodes into cortical tissue," *Ann. Biomed. Eng.*, vol. 20, pp. 413–22, 1992.

[13] A. Prochazka and M. Gorassini, "Ensemble firing of muscle afferents recorded during normal locomotion in cats," *J. Physiol.*, vol. 507, pp. 293–304, 1998.

[14] A. Prochazka and M. Gorassini, "Models of ensemble firing of muscle spindle afferents recorded during normal locomotion in cats," *J. Physiol.*, vol. 507, pt. 1, pp. 277–91, 1998.